Materials Science, *Vol. 21*, *No. 4*, *2003*

Electrochemical evaluation of protective properties of one-component SiO_2 and TiO_2 coatings obtained by the sol-gel method

EWA SZAŁKOWSKA[1*], JAN MASALSKI[2], JÓZEF GŁUSZEK[2]

[1]Department of Chemistry, Częstochowa University of Technology,
al. Armii Krajowej 19, 42-200 Częstochowa, Poland

[2]Institute of Inorganic Technology and Mineral Fertilizers, Wrocław University of Technology,
Wybrzeże Wyspiańskiego 27, 50-370 Wrocław, Poland

The paper presents the corrosion resistance of uncoated steel and steel coated with one-component films in 0.5 M H_2SO_4 at 22.0±0.2 °C. One-component coatings were obtained by the sol-gel method. The coatings were obtained by the dip coating method. Quantitative composition of the coatings and their thickness were estimated by means of X-ray Photoelectron Spectroscopy (XPS). The corrosion behaviour of steel coated with one-component films was evaluated with the use of electrochemical direct and alternating current methods.

Key words: *sol-gel method; XPS method; potentiodynamic curves; impedance*

1. Introduction

The main focus of research on corrosion-resistant materials nowadays is the modification of the surface layer. The most popular methods involve coating the metal or admixing some elements into it. The interest in ceramic coatings deposited on various materials has been increasing in recent years, due to such properties of the ceramics as high mechanical strength, high melting point, abrasion and corrosion resistance even in aggressive environments. The sol-gel technique applied to depositing ceramic films on materials has been gaining increasing recognition, as it offers wide possibilities of producing both one-component and multicomponent coatings [1–4]. Among other advantages of the sol-gel technique, one has to mention the control of microstructure of the coating films, their high purity and relatively low temperatures as compared to the conditions of obtaining solid ceramics.

[*]Corresponding autor, e-mail: ewas@mim.pcz.czest.pl.

The sol-gel coatings are used for protection against electrochemical and high-temperature corrosion [5–8]. The significance of the sol-gel technique in general is best evidenced by the variety of its applications for obtaining new materials in the form of fibres, films, powders, devitrificates, monolithic glass, ceramics, and, last but not least, coatings [9–14].

The aim of the present project is to obtain one-component coatings on chromium steel by means of the sol-gel technique, and to assess the protective properties of the coatings in the environment of 0.5 M H_2SO_4.

2. Experimental

The substrate was chromium steel which is a modification of the AISI 403 type. In the sol-gel method, one of the steps is a high-temperature treatment of oxide coatings. The steel substrate might show a phase transition during this operation if the iron steel is used. To avoid this, the chromium steel (modification of AISI 403) was chosen. The additional elements – molibdenium and vanadium (absent in AISI 403) stabilize the precipitated carbides making the steel more temper-resistant. For the chemical composition, see Table. The samples were in the form of discs 12.0 mm in diameter and 1.0 m thick. Before coating, the surfaces were ground with an emery paper #1000, rinsed with distilled water and degreased with tetrachloromethane in an ultrasound washer.

Table. Chemical composition of the stainless steel (% w/w)

C	Mn	Si	P	S	Cr	Ni	Mo	V	W	Cu
0.12	0.51	0.35	0.026	0.029	12.4	0.43	0.11	0.04	0.13	0.12

To obtain an SiO_2 sol, the solution containing 25.0 g of tetraethoxysilane $Si(C_2H_5O_4)$ and 11.0 g of anhydrous ethanol (C_2H_5OH) was used, to which another solution of 11.1 g of anhydrous ethanol and 8.6 g of distilled water was added. Subsequently, the solution obtained was stirred by means of a magnetic stirrer with a constant speed (300 r.p.m.) for one hour. Then, the solution was left in an open vessel at the temperature of 20 ± 5 °C, until the sol of required viscosity (about 3 cP) had been obtained. The time needed for obtaining the appropriate sol depends also on the factors affecting the ratio of solvent evaporation, i.e. the temperature, air humidity and circulation. In the sol obtained, the content of the coating material was 13% (m/m) with respect to SiO_2. The reaction of hydrolysis of the tetraethoxysilane (TEOS) proceeds in the following way:

$$Si(C_2H_5O)_4 + (2+n)\,H_2O \rightarrow SiO_2{\cdot}nH_2O + 4C_2H_5OH \qquad (1)$$

The viscosity of the solutions used for SiO_2 coatings was 3.3–3.4 cP, as measured with a Hoopler viscosimeter at 20 °C.

To obtain a TiO_2 sol, a solution containing 6.0 cm^3 of tetraisopropyl orthotitanate $Ti(C_3H_7O)_4$ and 45.0 cm^3 of anhydrous ethanol was used, to which a solution containing 6.0 cm^3 30% (m/m) of hydrous acetic acid and 45.0 cm^3 of anhydrous ethanol was added while stirring. The solution obtained was left in a closed vessel to age. After 3–5 hours the solution became turbid, yielding 2.0% (m/m) of TiO_2 sol. The reaction of the hydrolysis of tetraisopropyl orthotitanate proceeds as follows:

$$Ti(C_3H_7O)_4 + (2+n)\,H_2O \rightarrow TiO_2{\cdot}nH_2O + 4C_3H_7OH \qquad (2)$$

The viscosity of the solution at 20 °C was 3.4 cP as measured with a Hoppler viscosimeter.

The films were deposited on the substrates by dip coating. First, the sol was homogenized for 45 minutes in an ultrasound washer, then the samples were dipped in the sol for 2 minutes in order to establish equilibrium at the boundary of the substrate/solution phases. The dipping and withdrawing of samples was performed at a constant rate of 1.0 mm/s. The samples were then dried in the cool air for 24 hours, and heated in an electrical furnace, which was heated to the maximum temperature at the rate of 2.0 °C/min. The samples examined were coated with five layers of the film in such a way that the first four layers were heated at 500 °C for 10 minutes, and the fifth, external layer was heated at 750 °C for 30 minutes.

The one-component coatings obtained by means of the sol-gel method on the chromium steel were examined with a scanning microscope Cambridge Stereoscan SC-180.

The X-ray Photoelectron Spectroscopy was performed by means of an electron analyzer AMICUS (KRATOS Analytical). The coated samples were cut to the size of 5.0 mm^2, covered with a conducting tape on both sides, and placed in a vacuum chamber. The tape carried away the electrostatic charge from the samples, thereby minimizing shifts in the peaks of the bonds energy. The spectra were recorded using the pass energy of 75 eV and an X-ray energy of 240 W. The analysis of the surfaces was enhanced with a depth profile obtained by etching with a fast Kauffman ion Argon gun. The stable parameters of the gun operation ($p = 1\times10^{-2}$ Pa, emission current 100 mA, and acceleration voltage 200 V) enabled the scaling of the profile. Both etching of the samples surfaces and their analysis were performed at various locations on the films, which minimized the risk of damaging the surface. The quantitative analysis of the coatings was carried out with the original software of the AMICUS spectrometer.

Electrochemical examinations were performed with direct and alternating currents. Polarization curves were measured in a conventional three-electrode thermostated system which enabled maintaining constant temperature of 22.0±0.2 °C during the measurements. In the potentiodynamic tests a platinum electrode was used as the auxiliary one and a saturated calomel electrode (SCE) as the reference one. The analysis of the dependence of current density on the potential applied in a 0.5 M H_2SO_4 solution was performed by means of an automated measuring system consisting of a EP-20 potentiostate, an EC 20B generator, a 5D logarithmic amplifier (ELPAN, Poland)

and a system for signal recording (AMBEX, Poland) connected to a PC. The potential was changed from the cathodic to the anodic values with respect to the SCE, the rate of change being small (1.0 mV/s), since the passivation process is typically slow. Impedance spectroscopy was carried out with a HF FRA 1255 device (Schlumberger) connected to an impedance interface ATLAS 9181. The measuring system was controlled by an IBM PC program Imp-opt v. 4.0, through the GPIB interface. The impedance measurements were performed within a Faraday cage in order to reduce external interferences. The two-electrode arrangement enabled the measurements of impedance up to 1.0 GΩ. The platinum electrode was used as an auxiliary electrode. The upper limit of frequency was 3.0 kHz, whereas the lower limit was 0.001 Hz. The amplitude of the sinusoidal interference signal was 25.0 mV. The measurements were carried out at the corrosion potential occurring after various periods of exposure of the samples to the solution. Repeatability was checked by making two measurements for one sample, first starting at low frequencies and the second starting at high frequencies. The spectra were virtually identical, it can be thus concluded that the examined systems did not change during the measurements. The impedance spectra are presented in the Bode diagram system recorded at 22.0±0.2 °C. The resulting impedance spectra were numerically processed by an Equivalent Circuit (version 4.51) Boukamp program in order to obtain the best-fit values of the circuit elements.

3. Results and discussion

The surface topographies of one-component films are presented in Figs. 1, 2. In Figure 1, showing the surface of the TiO_2 coating, one can see uneven spherical grains of various sizes. The TiO_2 coating is non-homogeneous and cracked. The cracks probably result form contractions occurring during the process of drying and heating, even though the heating ratio was low (2 °C/min). The increase in the density of the coating at higher temperatures (above 700 °C) makes the crystalline layer of Cr_2O_3 thicker at the substrate/coating boundary, which may cause cracks at lower temperatures [15]. On the other hand, applying higher temperatures was necessary to remove excess of water adsorbed physically and chemically from the dried gel [16]. As evidenced in Fig. 2, the SiO_2 coating is also cracked.

The results of the XPS analyses are presented in Figs. 3, 4, where the contents of elements considered are functions of the etch time and the thickness of the substrate. The estimated thickness of the TiO_2 coating was approx. 600–800 nm (Fig. 3). In the whole profile of the TiO_2 coating, there are actually no peaks from the substrate, i.e. iron or chromium. Initially high concentration of carbon atoms in the film decreases rapidly, almost disappearing below 50 nm, thereby providing evidence for surface adsorption of the carbon compounds. Down to the depth of 600 nm the composition of the coating is stable, the oxygen concentration is approx. 50%, and titanium concentration is only slightly lower than that of oxygen – 42%. The gradual decrease in the titanium concentration can be ascribed to uneven thickness of the coating. One can

also observe an increase in the chromium concentration associated with its diffusion towards the surface, occurring during the high-temperature treatment. Chromium is present in the oxidized form (Cr_2O_3), hence a small increase in the oxygen concentration is observed. Manganese present on the surface comes from the steel substrate. Its concentration seems to be out of proportion as compared to that of other elements

coming from the substrate. This is caused by the process of surface segregation occurring during steelmaking.

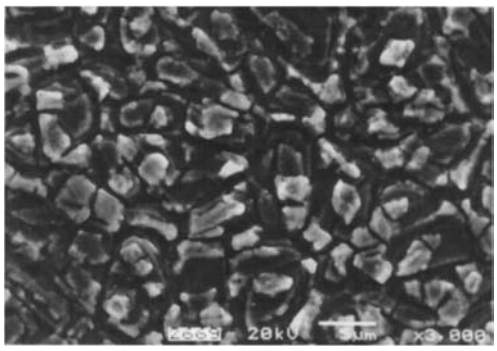

Fig. 1. Microstructure of the TiO_2 film on the chromium steel surface

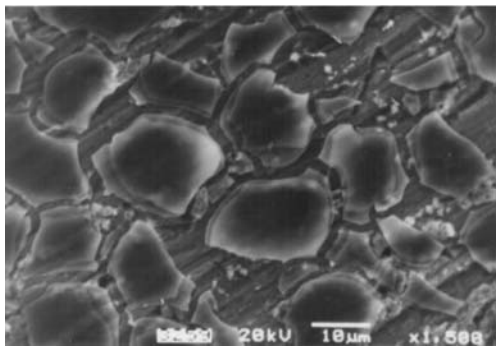

Fig. 2. Microstructure of the SiO_2 film on the chromium steel surface

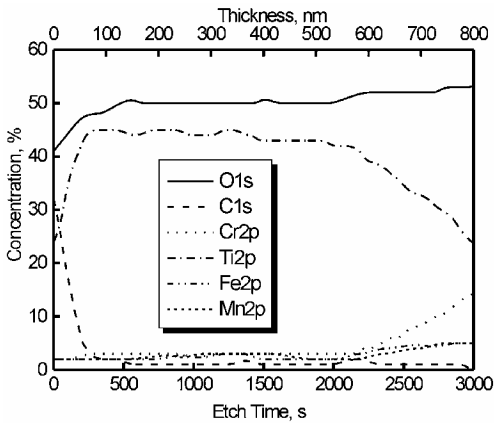

Fig. 3. Depth profile of the TiO_2 film on the chromium steel surface

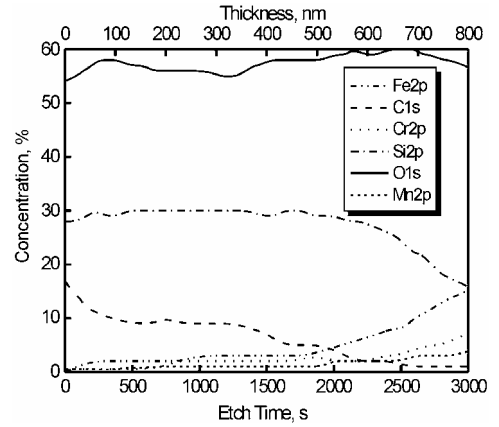

Fig. 4. Depth profile of the SiO_2 film on the chromium steel surface

The thickness of silica layer covering the steel substrate was estimated as about 800 nm (Fig. 4); it is therefore relatively thick. Down to 600 nm the silicon concentration is constant, at the level of 30% (Fig. 4, line Si2p). The coating is characterized by a high carbon content in all its volume. The surface layer is of organic origin and builds into the structure of the silica coating in the process of the high-temperature treatment. The ultimate drop of the carbon concentration is caused by the decrease in silicon concentration, the two being probably bound. The coating is homogeneously

oxidized throughout all its thickness, the concentration of oxygen is maintained at the level of 55–60% (Fig. 2, line O1s). Interestingly, no diffusion of chromium towards the surface has been observed, therefore the iron concentration exceeds the chromium concentration throughout the depth of the coating.

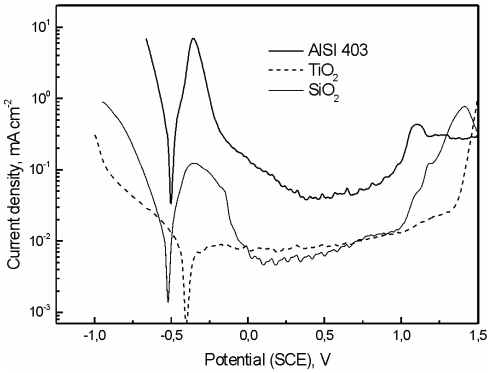

Fig. 5. Potentiodynamic curves for steel samples, uncoated and coated with the SiO_2 and TiO_2 films, in 0.5 M H_2SO_4

Effectiveness of the oxide layers was assessed by the polarization measurements carried out in 0.5 M H_2SO_4. As can be clearly seen in the polarization curves shown in Fig. 5, both the cathodic and anodic current densities are significantly lowered by the coatings. The rate of the anodic process at the corrosion potential for the TiO_2 and SiO_2 coatings is reduced by approx. two orders of magnitude as compared to the steel surface. The comparison of various one-component coatings (Fig. 5) indicates that the best barrier against corrosion is provided by the 5-layer TiO_2 coating.

The results of the impedance measurements recorded on the uncoated and coated steel samples are presented in Fig. 6 as the Bode diagrams for various periods of exposure to the H_2SO_4 solution. The impedance spectra obtained for the uncoated steel differ significantly from those obtained for the coated samples. The value of the impedance module is higher for the coated steel, indicating its higher chemical resistance to the corrosive solution.

The 'Equivalent-Circuit' program (Boukamp) was used for developing electrical equivalence models for the bare steel (Figs. 7a, 7b) and for the one-component coatings (Fig. 7c). The program gave a good match between the calculated spectra and the spectra obtained experimentally. The impedance spectra recorded for the steel exposed to the 0.5 M solution of H_2SO_4 obtained after exposure periods ranging from 10 minutes to 4 hours correspond to the equivalent model R1(R2Q3) (Fig. 7a). In this model, R1 represents the resistance of the electrolyte and of the products of the film corrosion, R2 is the resistance of the charge transfer, and Q3 models the electrical double layer by means of the so-called constant-phase element.

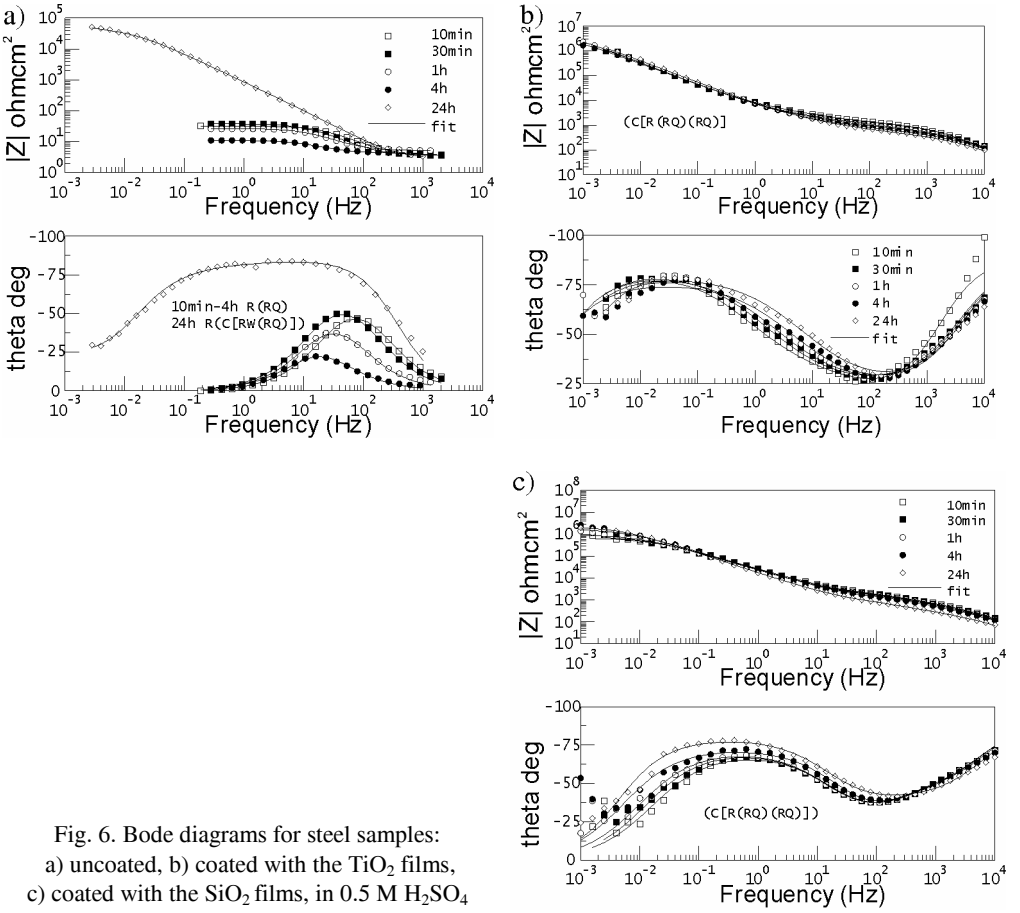

Fig. 6. Bode diagrams for steel samples:
a) uncoated, b) coated with the TiO_2 films,
c) coated with the SiO_2 films, in 0.5 M H_2SO_4

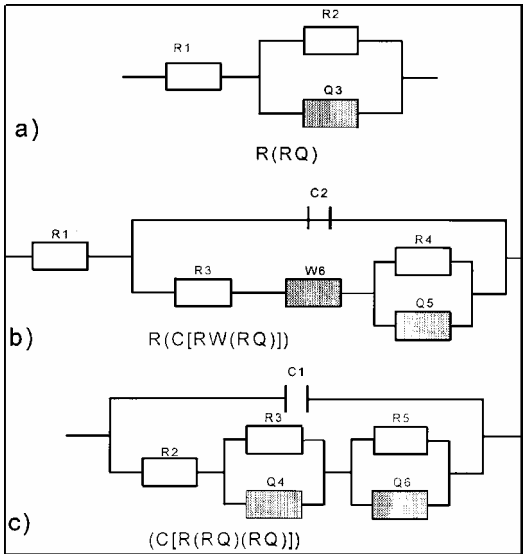

Fig. 7. Electrical equivalent circuits for uncoated steel (a, b) and the steel coated (c) in 0.5 M H_2SO_4

Extending the exposure time to 24 hours renders the R1(R2Q3) equivalent circuit, obtained by means of the Boukamp circuit description mode, inadequate. The spectrum obtained after 24-hour exposure of the steel samples to the acidic solution exhibits high low-frequency impedance module and high constant value of the phase angle within the broad range of frequencies, the latter probably resulting from joining two maxima of the phase angle (Fig. 6a).

The occurrence of the two inseparable maxima of the phase angles is a consequence of an additional element appearing in the electrical equivalent circuit. Figure 7b presents a circuit generating an impedance spectrum correlating with the experimental spectrum. The elements R1, R4, and Q5 in Figure 7b correspond to R1, R2, Q3 in Fig. 7a. Element C2 is the capacitance of the corroded layer adhering tightly to the steel surface, elements R3 and W6, are the resistance of the electrolyte in the pores of the corroded layer and Warburg pseudo-impedance associated with diffusion processes, respectively.

The best fit between the simulated spectra of the coated steel and the experimental ones is obtained with the use of the (C[R(RQ)(RQ)]) model of the electrical equivalent circuit, presented in Fig. 7c. This model is very similar to the one used in the description of stainless steel 304 coated with CeO_2 film exposed to a 1.0 M solution of NaCl [17]. The model presented in Fig. 7c contains additionally the element C1 (electrode capacitance) [18]. The physical sense of the elements R2, R5, and Q6 presented in Fig. 7c is identical to that of the elements R3, R4, and Q5 in Fig. 7b. The elements R3 and Q4 in Fig. 7c are connected to certain properties of the coatings and denote, a resistive element and a constant-phase element, both characterizing electrical properties of the passive layer.

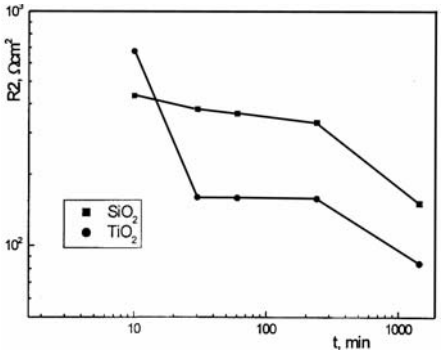

Fig. 8. Resistance of the electrolyte in through -coatings pores (R2) versus exposure time of SiO_2- and TiO_2-coated steel

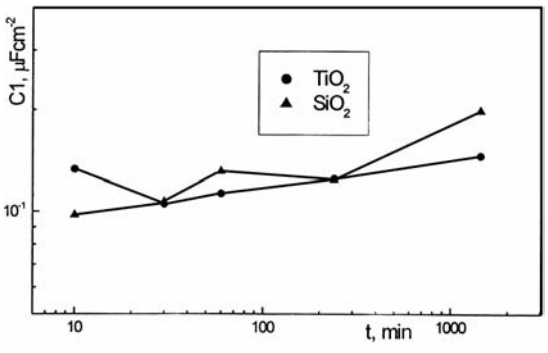

Fig. 9. Capacitance of coatings (C1) versus exposure time of SiO_2- and TiO_2-coated steel

On one hand, the use of two constant-phase elements in the electrical equivalent circuit facilitates the match between the calculated and experimental curves. On the other hand, it introduces four additional parameters, whose physical sense cannot be

easily determined. In spite of this complication, the model developed adequately reflects the physical properties of the investigated system: metal–coating–electrolyte.

In Figure 8, changes in the R2 value of the TiO_2 and SiO_2 coatings are presented as a function of the exposure time to the corrosive solution. As the exposure time increases, the conductivity of the solution also increases (i.e. the resistance decreases), indicating appearance of micro-cracks and new conduction paths (or broadening of the existing ones). The changes in the capacitance (C1) of the coating film typically result from the penetration of water. Water affects the dielectric constant of the coating and, consequently, increases its capacitance. The changes in capacitance of the samples immersed in the corrosive solution are presented in Fig. 9. The capacities of the TiO_2 and SiO_2 coatings increase during the exposure to the 0.5 M H_2SO_4 solution, possibly indicating that the penetration by water is preceded by a several-hour period of induction. The capacitance of the SiO_2 coating is higher than that of the TiO_2 coating. The value of Q6 reflects the degree of delamination of the coating. The fact that this parameter does not show any significant variation over time (Fig. 10) means that no delamination occurs. The decrease in the value of Q6 with the time of exposure in the case of the TiO_2 coating can result from diminishing the metal surface being in contact with the electrolyte through pores and cracks. From the point of corrosion protection, the most crucial parameter is the charge transfer resistance (R5) (Fig. 11) which is inversely proportional to the corrosion rate and to the area corroded. The increase in the value of R5 can be attributed to the process of reconstruction of the internal layer or to the process of 'self-repair' occurring in the layer. In the case of the TiO_2 and SiO_2 coatings, the value of R5 increases, depicting continuous inhibition of corrosion.

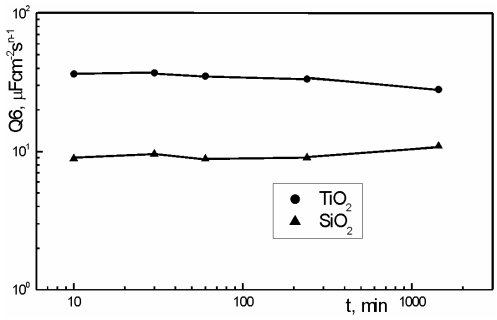

Fig. 10. Constant phase element (Q6) versus exposure time of SiO_2- and TiO_2-coated steel

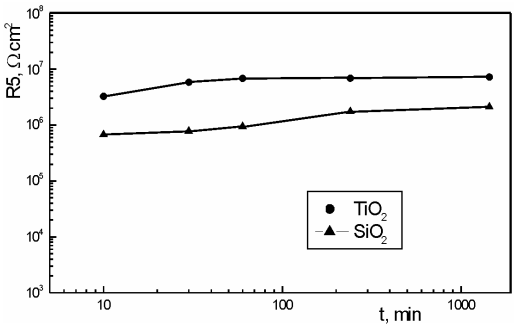

Fig. 11. Charge transfer resistance (R5) versus exposure time of SiO_2- and TiO_2-coated steel

The analysis presented above indicates that the corrosion processes occurring in the systems of coatings obtained by the sol-gel method on chromium steel are of a highly complex nature. It has to be also noted that the TiO_2 and SiO_2 coatings are not electrical barriers and that their defects cause considerable scatter of the results.

4. Conclusion

It is possible to obtain one-component coatings on chromium steel by means of the sol-gel method. The TiO_2 and SiO_2 coatings, enhancing the corrosion resistance in the environment of 0.5 M H_2SO_4, are about 800 nm thick. The one-component coatings are non-homogeneous, with many cracks (Figs. 1, 2). The cracks probably result from contractions occurring during the process of drying and heating. The impedance measurements indicate that the coatings are poor barriers due to the presence of numerous cracks through which charge transfer can occur.

References

[1] BRINKER C.J., SCHERER G.W., *Sol-gel: the physics and chemistry of sol-gel processing*, Academic Press, San Diego, 1990.
[2] KLOTZ M., AYRAL A., GUIZARD C., COT L., Bull. Korean Chem. Soc., 20 (1999), 879.
[3] KUNDU D., BISWAS P.K., GANGULI D., J. Non-Cryst. Solids, 110 (1989), 13.
[4] ANDRIANOV K.A., *Organic Silicon Compounds* (in Russian), Gos. Nauchno-Tekhn. Izd. Khim. Lit., Moscow, 1955.
[5] ATIK M., DE LIMA NETO P., AEGERTER M. A., AVACA L. A., J. Appl. Electrochem., 25 (1995), 142.
[6] ATIK M., ZARZYCKI J., J. Mat. Sci. Letters, 13 (1994), 1301.
[7] VASCONCELOS D.C.L., CARVALHO J.A.N., MANTEL M., VASCONCELOS W.L, J. Non-Cryst. Solids, 273 (2000), 135.
[8] GŁUSZEK J., MASALSKI J., ZABRZESKI J., NITSCH K., GŁUSZEK P., Thin Solid Films, 349 (1999), 186.
[9] MAKISHIMA A., OOHASHI H., WAKAKUWA M., J. Non-Cryst. Solids, 42 (1980), 545.
[10] KAMIYA K.,. SAKKA S., TATERNICKI T, J. Mater. Sci., 15 (1980), 1765.
[11] MAKISHIMA A., ASAMI M., WADA K., J. Non-Cryst. Solids, 121 (1990), 310.
[12] ANDERSON M.L., STROUD R.M., MORRIS C.A., MERZBACHER C.I., ROLISON D.R., Adv. Eng. Materials, 8 (2000), 481.
[13] GARBASSI F., BALDUCCI L., UNGARELLI R., J. Non-Cryst. Solids, 223 (1998), 190.
[14] HOLMES-FARLEY S. R., YANYO L. C., Adhesion Sci. Technol., 5 (1991), 131.
[15] ATIK M., MESSADDEG S.H., LUMA F.P., AEGERTER M.A., J. Mat. Sci. Letters, 15 (1996), 2051.
[16] HENCH L.L., WANG S.H., Phase Trans., 24 (1990), 785.
[17] BISWAS R.G., SANDERS R.D., J. Mat. Eng. Perf., 7 (1998), 727.
[18] JUTTNER K., Electrochim. Acta, 35 (1990), 1501.

Received 15 June 2003
Revised 9 August 2003